

## Doubly Tuned Local Coils for MRI and MRS at 1.5 T\*

THOMAS M. GRIST,† A. JESMANOWICZ, J. BRUCE KNEELAND,  
W. FRONCISZ,‡ AND JAMES S. HYDE

*Department of Radiology, Medical College of Wisconsin, 8701 Watertown Plank Road,  
Milwaukee, Wisconsin 53226*

Received February 13, 1987; revised November 6, 1987

We describe a doubly tuned radiofrequency (RF) local coil probe designed specifically for performing *in vivo* image-localized spectroscopy. The probe was designed using principles developed in connection with the counter-rotating-current (CRC) and planar-pair loop gap resonators for magnetic resonance imaging (MRI). The probe design satisfies several criteria useful for *in vivo*  $^1\text{H}/^{31}\text{P}$  experiments at 1.5 T. First, sensitivity on the low-frequency mode is preserved relative to a singly tuned coil. This result was confirmed by bench-test and *in vitro* MR experimental data. Second, through principles of intrinsic decoupling the probe is isolated from any externally applied uniform excitation field, which is desirable for *in vivo*  $^1\text{H}$  imaging and solvent suppression. Third, the regions of sensitivity of the high- and low-frequency modes of the coil are similar, and therefore spectroscopic volumes of interest identified on an image will reflect the same volumes as those selected during spectroscopy. Finally, interface to the MR system is such that the high- or low-frequency circuits may be selected entirely under software control, with no requirement for changing coils or cables or moving the subject. © 1988 Academic Press, Inc.

The application of magnetic resonance imaging (MRI) and spectroscopy (MRS) to *in vivo* systems has developed rapidly since Hoult *et al.* demonstrated  $^{31}\text{P}$  spectra from muscle (1). Currently, there is much interest in performing *in vitro* and *in vivo* MRS experiments on nuclei including  $^1\text{H}$ ,  $^{31}\text{P}$ ,  $^{23}\text{Na}$ ,  $^{19}\text{F}$ , and  $^{13}\text{C}$ . In addition, many of the localization techniques described for *in vivo* MRS require acquisition of a proton image prior to collecting a spectrum from the volume of interest (2-4). These experiments dictate the use of either singly tuned radiofrequency (RF) coils which are repositioned over the sample for different nuclei or RF coils tuned to multiple frequencies. Doubly tuned NMR receiver coils have been described for *in vitro* (5, 6) and recently for unlocalized *in vivo* MRS by several investigators (7-10). However, these RF probe designs have in general compromised sensitivity on the low-frequency resonance mode in order to obtain more than one resonance. In addition, techniques useful for *in vivo* MRS, proton imaging, gradient-localized spectroscopy, and solvent

\* Presented at the 5th Annual Meeting of the Society of Magnetic Resonance in Medicine, Montreal, 1986.

† Present address: Department of Radiology, Duke University Medical Center, P.O. Box 3808, Durham, NC 27710.

‡ On leave from the Department of Biophysics, Institute of Molecular Biology, Jagiellonian University, Krakow, Poland.

suppression place unique demands on multiple-resonance RF coils not addressed by previous investigators. For example, the ability to operate in an externally applied relatively uniform transmit field is important for imaging and solvent suppression. We define several criteria as essential characteristics of a doubly tuned RF probe used for  $^1\text{H}$  imaging,  $^1\text{H}$  solvent suppressed MRS, and gradient-localized  $^{31}\text{P}$  MRS on a large-bore (70-cm) clinical MR system operating at 1.5 T: (1) sensitivity on the low-frequency mode should be preserved. (2) Loss of sensitivity on the high-frequency mode can be tolerated to a greater extent because of the increased  $^1\text{H}$  sensitivity *in vivo*, in addition to the fact that sample losses dominate the expression for coil quality factor at higher frequencies. (3) Coil modes should be decoupled from any externally applied uniform excitation field. (4) The coil modes should have similar field distributions for accurate image-based localization of spectra.

We describe a doubly tuned RF local probe which satisfies the aforementioned criteria. The coil was developed in connection with loop-gap resonator design principles for MRI and electron spin resonance (ESR) spectroscopy (11-14). The architecture of the coil and its interface to the G.E. Signa imager is shown in Fig. 1 and is such that all coil resonances are decoupled (electrically isolated) from each other. Thus, the following sequence is possible, without changing coils, for *in vivo* spectroscopy: (1) the probe is placed over the area of interest and is tuned for that sample; (2) a localizer image is obtained using the body coil to transmit and the doubly tuned probe in receive only mode; (3) the  $B_0$  field homogeneity is adjusted over the gradient-localized region of interest by observing the  $\text{H}_2\text{O}$  FID; (4) proton spectra are acquired; and (5)  $^{31}\text{P}$  spectra are acquired using the local transmit coil for excitation and the low-frequency mode of the doubly tuned receiver coil for reception.

#### METHODS

The probe is a local coil transmit/receive pair consisting of a small doubly tuned (25.8/63.9-MHz) receiver coil and a singly tuned (25.8-MHz) transmit coil. Specifically,

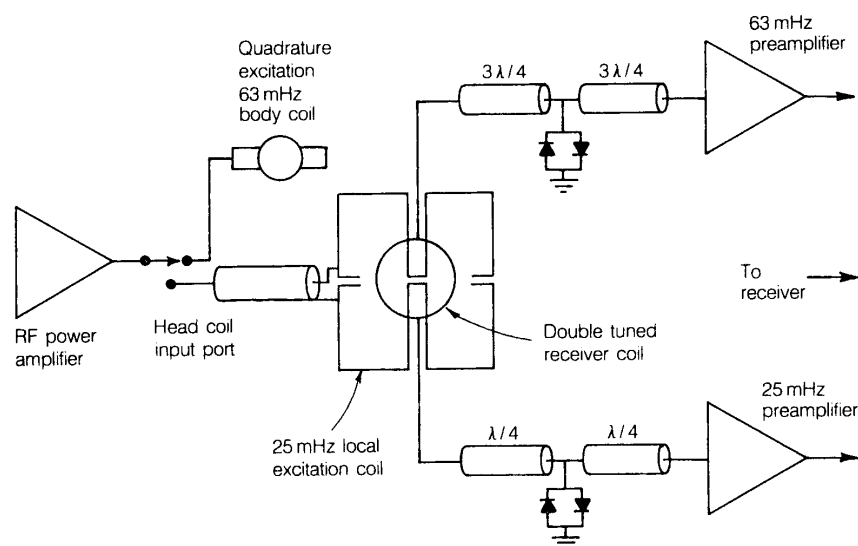


FIG. 1. Block diagram of the interface between doubly tuned local coil and MR system.

the doubly tuned receiver coil was designed using principles developed in connection with the counter-rotating-current (CRC) loop-gap resonator (13). Two resonators, coaxial and separated by distance ( $L$ ), will give rise to two resonant modes (Fig. 2). In the CRC coil for MR imaging, the lower-frequency mode is suppressed. In the doubly tuned coil, however, this mode is tuned to the lower-frequency ( $^{31}\text{P}$ ,  $^{23}\text{Na}$ ,  $^{13}\text{C}$ ) resonance at 1.5 T. The frequency ratio is governed by the mutual inductance between the loops and the value of the coupling capacitance,  $C_3$ . The equivalent circuit is shown in Fig. 3 where  $C_3$  is the coupling capacitance,  $L_1C_1$  and  $L_2C_2$  are the resonance elements, and  $C'_2$  and  $C'_3$  tune the high- and low-frequency modes, respectively.

Construction techniques similar to those previously described for NMR loop-gap resonators were used. The doubly tuned receiver coil is fabricated using copper strip (3M, 1151) wound on the inside of 3-in.-diameter PVC pipe (Fig. 4). The capacitive gaps are formed from etched microwave circuit board (RT/Duroid  $\epsilon = 10.2$ , 0.254 mm thickness). The coupling capacitor is also etched onto the microwave circuit board. Nonferrous trimmer capacitors are soldered in parallel with  $C_2$  and  $C_3$  in order to tune the high-frequency and low-frequency modes, respectively.

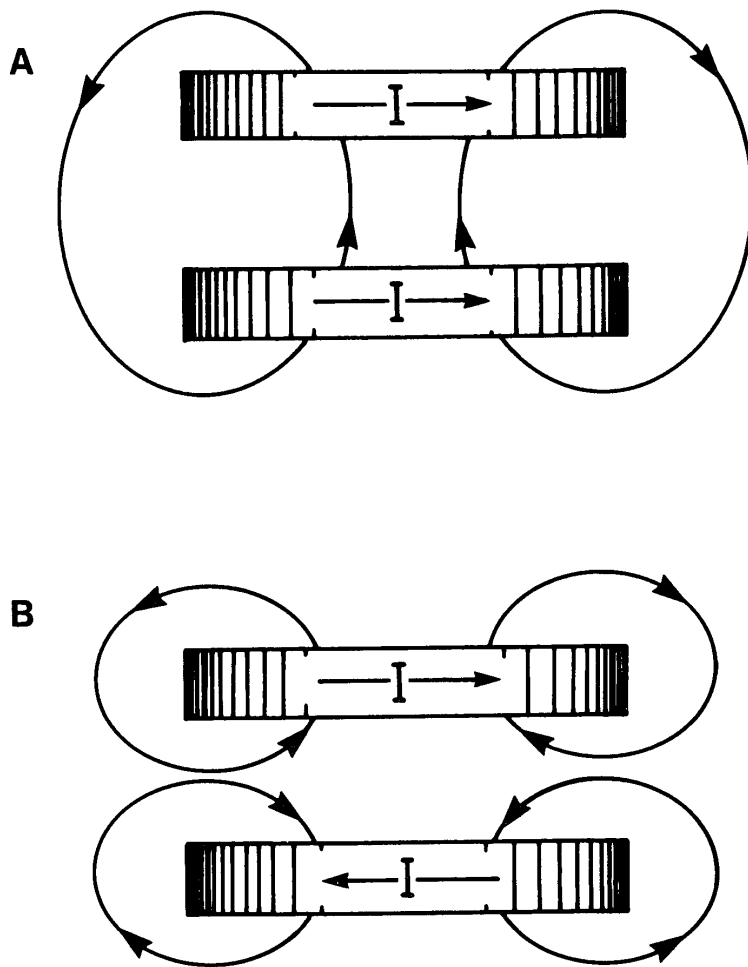


FIG. 2. Resonant modes of conductive loops with mutual inductance ( $M$ ). (A) Parallel current low-frequency mode; (B) antiparallel (counter-rotating)-current high-frequency mode.

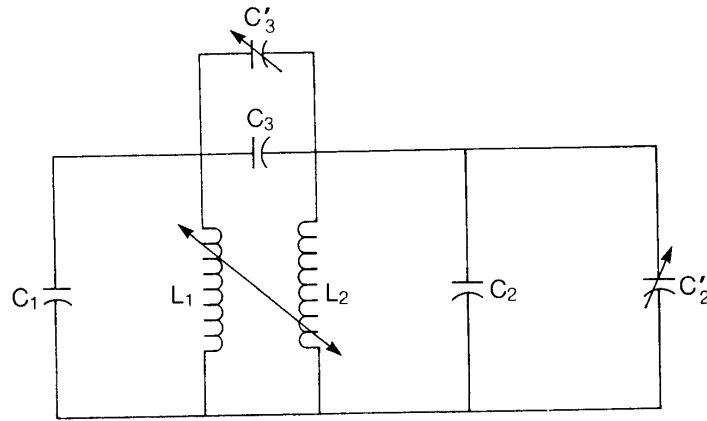


FIG. 3. Equivalent circuit for doubly tuned coil. Symbols as in text.

Inductive coupling is used to match the coil to the 50-ohm transmission line (14). Coupling can be achieved either by a single transmission line and inductive loop coupled to both modes or by two transmission lines and electrically isolated coupling loops coupled to each mode independently. In the former case, match is accomplished by varying the angle and displacement of the loop with respect to the resonator, while in the latter situation, match is achieved by adjusting the size of the coupling loops and variable capacitors at one-quarter wavelength from the loops. The loops are positioned geometrically to couple each mode independently and to have no mutual inductance (isolation 49 dB) (Fig. 5).

The transmit coil is a distributed capacitance planar-pair loop-gap resonator (Fig. 6). The coil is fabricated from copper strip (3M) wound on the inside of an 8-in. PVC pipe, 1 in. high. The circumference of the coil is bifurcated by the conductive elements of the planar pair at a distance ( $S$ ) to obtain a uniform transmit field distribution in a plane parallel to the plane of the coil. The coil is tuned with distributed capacitance formed from etched microwave circuit board. The coil is coupled capacitively to the transmission line via one of the gaps in the distributed capacitance network. The

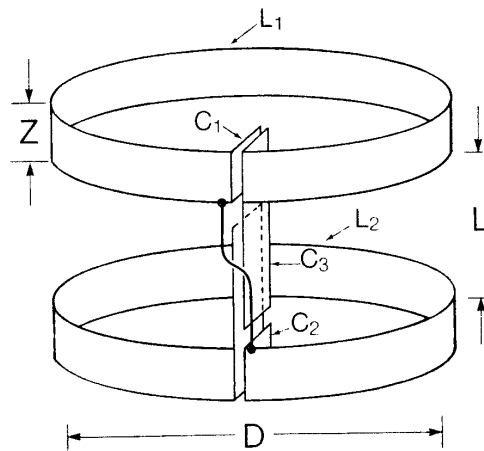


FIG. 4. Line drawing of resultant doubly tuned resonator.

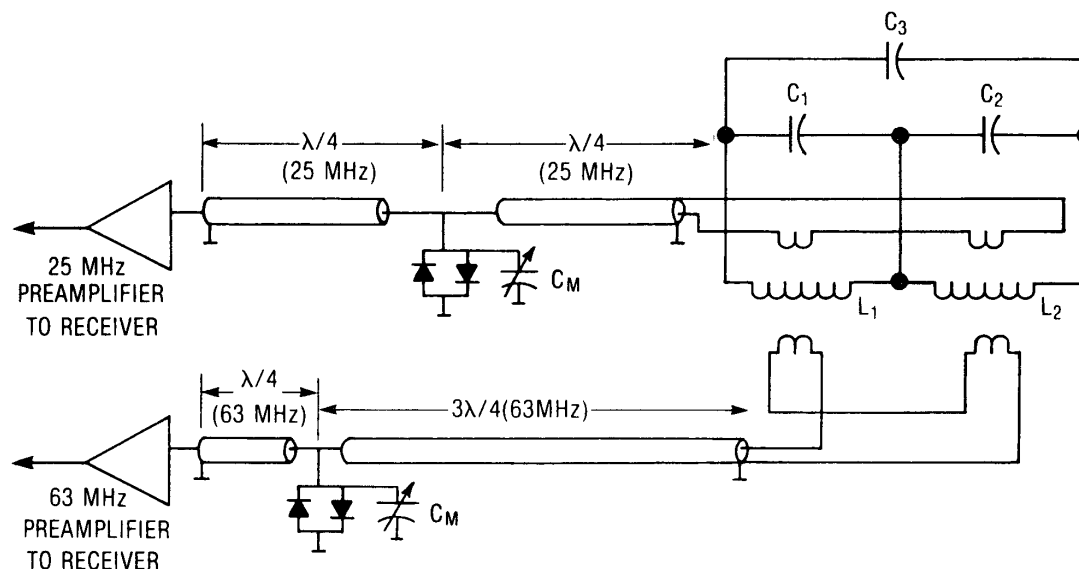


FIG. 5. Inductive coupling to the doubly tuned coil. Coupling is achieved with independent orthogonal coupling loops. Match to the transmission line is accomplished by varying capacitor  $C_M$  at  $\lambda/4$  wavelengths from coupling loop.

values  $C_1$ – $C_2$  are adjusted for each anatomic location (i.e., abdomen, thorax) to assure that tuning and matching the transmit coil for each patient are not required.

In order to minimize mutual inductance between all transmit and receive coil modes, the probe is configured as shown in Fig. 6. The high-frequency (CRC) mode of the receiver coil is decoupled from any externally applied uniform transmit field by principles of intrinsic decoupling described elsewhere (13). We use the body coil on the MR system to provide a relatively uniform excitation field. In addition, the low-frequency (25.8-MHz) mode of the doubly tuned receiver coil is decoupled from the local (25.8-MHz) transmit coil by principles of intrinsic decoupling. If the receive coil is precisely positioned in the geometric center of the transmit coil, flux arising from one loop of the excitation coil gives rise to EMFs in the receiver coil which cancel EMFs generated by flux from the opposite loop of the transmit coil.

Computer calculations of the transmit and receive field distributions were obtained using the Biot–Savart law and assuming uniform current distributions in the conductors. Coil quality factors ( $Q$ ), resonant frequency data, and field distribution data were obtained in the laboratory using techniques discussed previously (11–13). Loaded coil  $Q$  and sensitivity data were determined while loading the coil with solutions of 100 mM NaCl. All bench-test coil sensitivity measurements were made using a radiating dipole placed at varying distances from the coil in a 100 mM NaCl tank, as described elsewhere (12).

NMR experiments were performed on the G.E. Signa MR imager operating at 1.5 T. All spectra were obtained using pulse sequences commercially available through the G.E. Spectroscopy Research Accessory (SRA). Approval for human studies was obtained through the MCW IRB and informed consent was obtained in all cases.

*In vitro* NMR coil sensitivities were determined using a 7-cm-diameter phantom filled with 0.1 M  $H_3PO_4$ . The *in vitro* sensitivity of the doubly tuned coil was compared

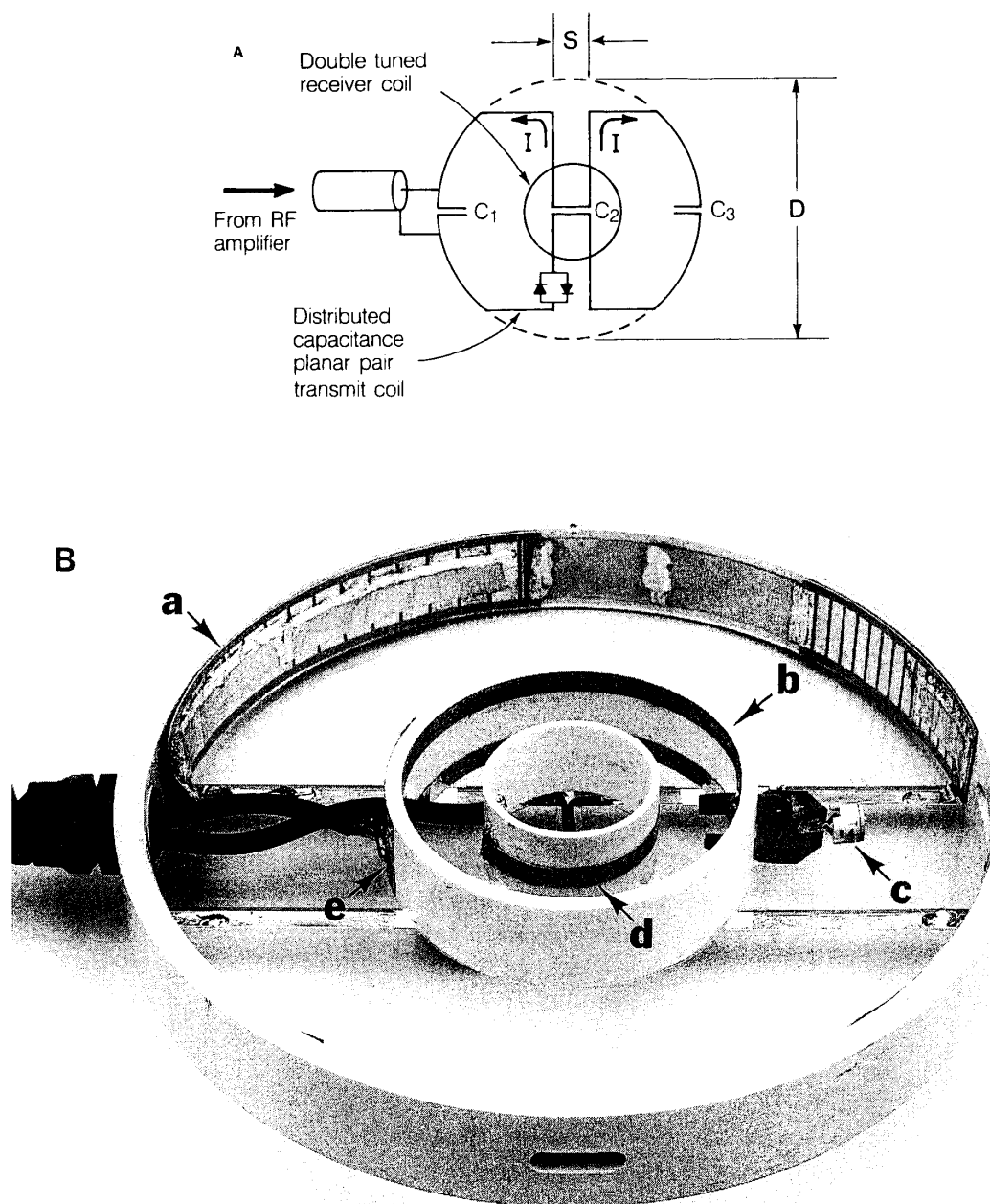


FIG. 6. (A) Line drawing of intrinsically decoupled transmit/receive pair. (B) Photograph of doubly tuned probe. (a) Distributed capacitance transmit coil. (b) Doubly tuned receiver coil. (c) Receiver coil tuning capacitors. (d) Low-frequency (25.8-MHz) receiver coil coupling loop. (e) High-frequency (63-MHz) receiver coil coupling loop seen on edge. Note position of receiver coil along the midline of the planar-pair transmit coil.

to that of a singly tuned coil of similar geometry (GE P31 spectroscopy coil). The single-frequency coil consisted of a 7.5-cm-diameter single-turn receiver and a 21-cm-diameter transmitter in a coplanar arrangement. The coils were electronically decoupled using active PIN diodes (15).

TABLE 1

Radiofrequency Characteristics of Single- and Double-Resonance Local Coils

	Low frequency (25.8 MHz)		High frequency (63.9 MHz)	
	$Q_0$	$Q_L$	$Q_0$	$Q_L$
Single-resonance Coil	304	89	260	110
Double-resonance Coil	288	85	230	114

Note.  $Q_L$ ,  $Q$  measured when coil is placed on 100 mM NaC phantom.

## RESULTS

Table 1 shows the quality factors ( $Q$ ) for each mode of a 3-in.  $^{31}\text{P}/^1\text{H}$  doubly tuned coil and typical values for singly tuned coils of similar geometries.  $Q_0$  is the unloaded  $Q$  measured with the coil in free space as described previously, while  $Q_L$  is the  $Q$  measured when the coil is placed adjacent to a physiologically equivalent saline phantom (11).

Tuning the coil is accomplished by using  $C_1$  and  $C_2$  to adjust the high-frequency and low-frequency modes independently. Tuning is unidirectionally noninteractive; i.e., if the high-frequency mode is tuned first, there is little perturbation in the resonance frequency of this mode when the low-frequency resonance is adjusted.

Results of the bench-test receive coil sensitivity determinations indicate that the sensitivity of the low-frequency mode of the doubly tuned coil is preserved relative to a singly tuned coil at the same frequency. Figure 7A shows the on-axis sensitivity vs distance from the coil for the low-frequency mode of the doubly tuned receiver coil

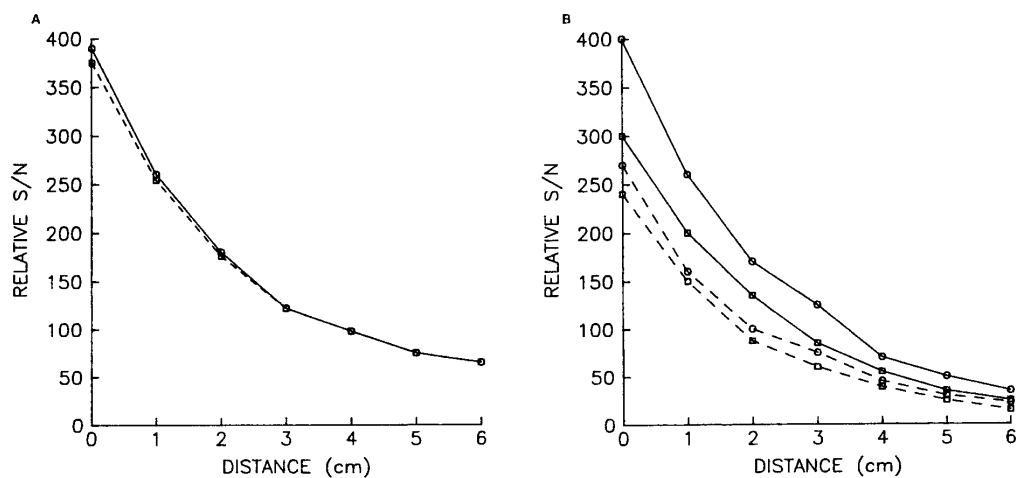


FIG. 7. Sensitivity profiles for single-resonance (○) and doubly tuned (□) coils. (A) Relative  $S/N$  vs distance from the coil for the low-frequency 25-MHz mode of the doubly tuned coil compared to a singly tuned single loop coil of the same size. (B) Relative  $S/N$  for the high-frequency mode (63-MHz) of the doubly tuned coil compared to a singly tuned (63-MHz) coil of the same diameter; (—) on-axis sensitivity; (---)  $S/N$  measured 4 cm off axis.

and for a typical high  $Q$  singly tuned loop-gap resonator. It is clear that there is little sensitivity difference between the low-frequency mode of the doubly tuned coil and a typical singly tuned high- $Q$  coil. However, the sensitivity of the low-frequency mode is preserved at the expense of the sensitivity of the high-frequency mode. Figure 7B shows the on-axis sensitivity of the high-frequency (CRC) mode of the doubly tuned coil relative to a singly tuned CRC LGR. The on-axis sensitivity is reduced at all points by approximately 20%.

The distance between the center conductors of the planar-pair excitation coil can be chosen to obtain a uniform field distribution in a plane parallel to the plane of the receiver coil. The uniformity was measured to be within  $\pm 3\%$  over the region of sensitivity of the 7.5-cm-diameter surface coil in a plane parallel to the coil. This is desirable in image-localized spectroscopy since the ROS defined on the image and determined by the ROS of the receiver coil in the uniform transmit field of the body coil will reflect the same ROS of the  $^{31}\text{P}$  transmit/receive coil pair. Second, for DRESS spectroscopy (2), since a large excitation coil is used, the transmit  $B_1$  field gradient across the thickness of the slice or along the axis of the coil is reduced, giving improved SNR for a selected slice in the coronal plane relative to the coil.

The intrinsic decoupling of the transmit/receive pair was verified when the receiver coil was positioned with respect to the transmit coil as in Fig. 6, for there is 49 dB isolation between the two coils. This is reduced to 45 dB when the pair is placed on the body, presumably due to RF field asymmetries introduced by the body.

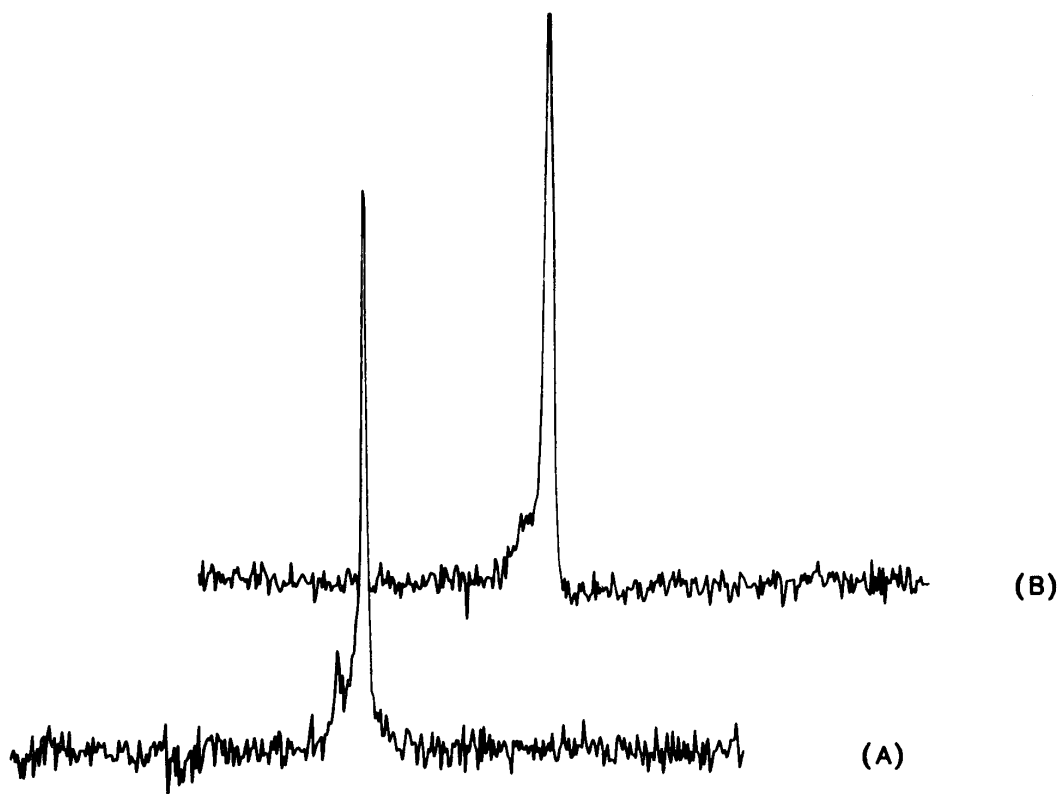


FIG. 8. NMR sensitivity comparison. (A) Commercially available single-resonance coil. (B) Doubly tuned coil described.



The bench-test measurements of the  $^{31}\text{P}$  sensitivity were confirmed by measurements on *in vitro* and *in vivo* samples. Figure 8A shows a  $^{31}\text{P}$  MR spectrum acquired from a 12.5-mm slice parallel to the plane of a 7.5-cm-diameter receiver coil and located 2 cm from the coil. The spectrum was acquired using the DRESS technique on a 7.0-cm-diameter bottle containing 100 mM  $\text{H}_3\text{PO}_4$  by averaging 20 excitations at 1000 ms repetition time. The SNR is 31.8. Figure 8B shows a  $^{31}\text{P}$  spectrum acquired under identical conditions using a commercially available singly tuned  $^{31}\text{P}$  MR receiver coil. The SNR is 26.5, giving a difference of 21.8%.

Finally, Fig. 9 shows an image of the human brain obtained by applying the doubly tuned LGR to the head under the occiput. The line drawn through the image defines the position of a 10-mm proton slice over which the static field homogeneity is adjusted ( $\text{H}_2\text{O}$  peak FWHM = 0.12 ppm) (Fig. 10A). A solvent suppressed proton spectrum is shown in Fig. 10B. The spectrum was collected using a spin-echo  $90^\circ\text{-TE}/2\text{-}180^\circ\text{-}$

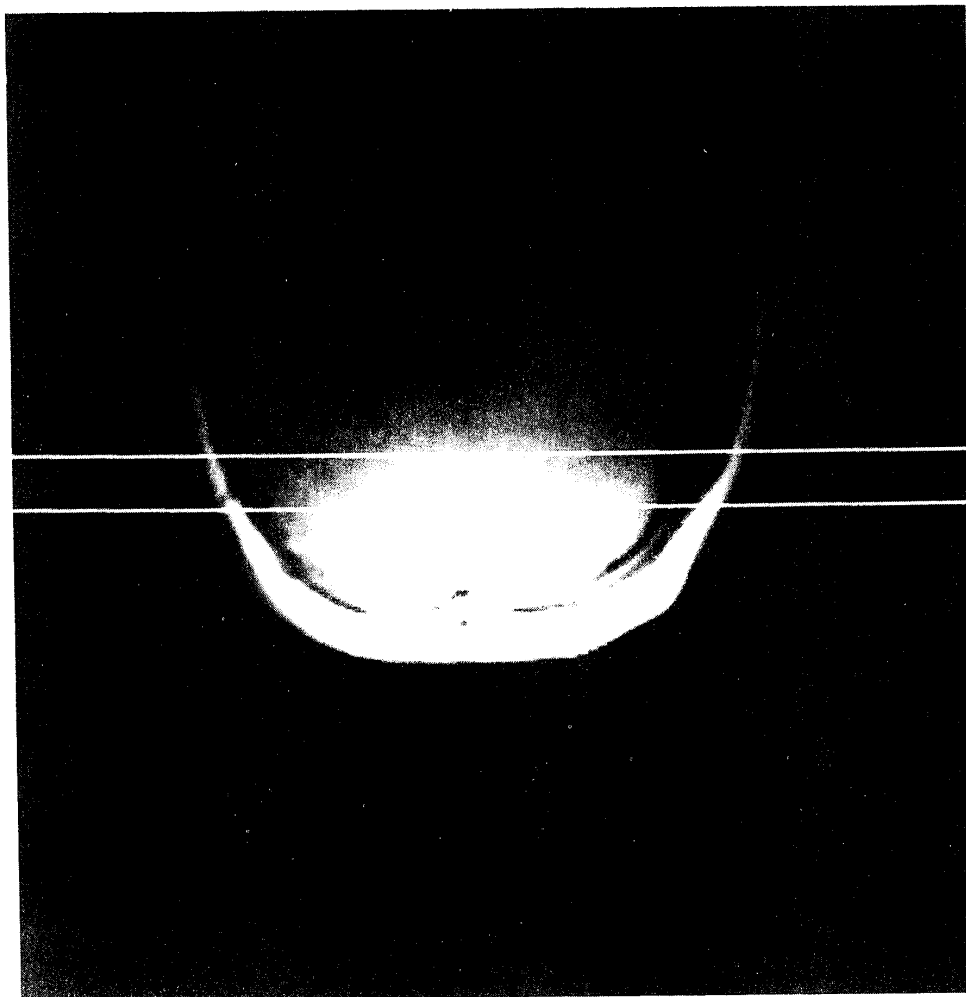


FIG. 9. Axial localizer image of the brain in a normal volunteer obtained using the high-frequency mode of the doubly tuned probe. The cursors drawn on the image define the thickness and location of a gradient-selected plane positioned within the brain. The spectroscopic volume of interest is defined by the intersection of the plane and the region of sensitivity of the doubly tuned probe.

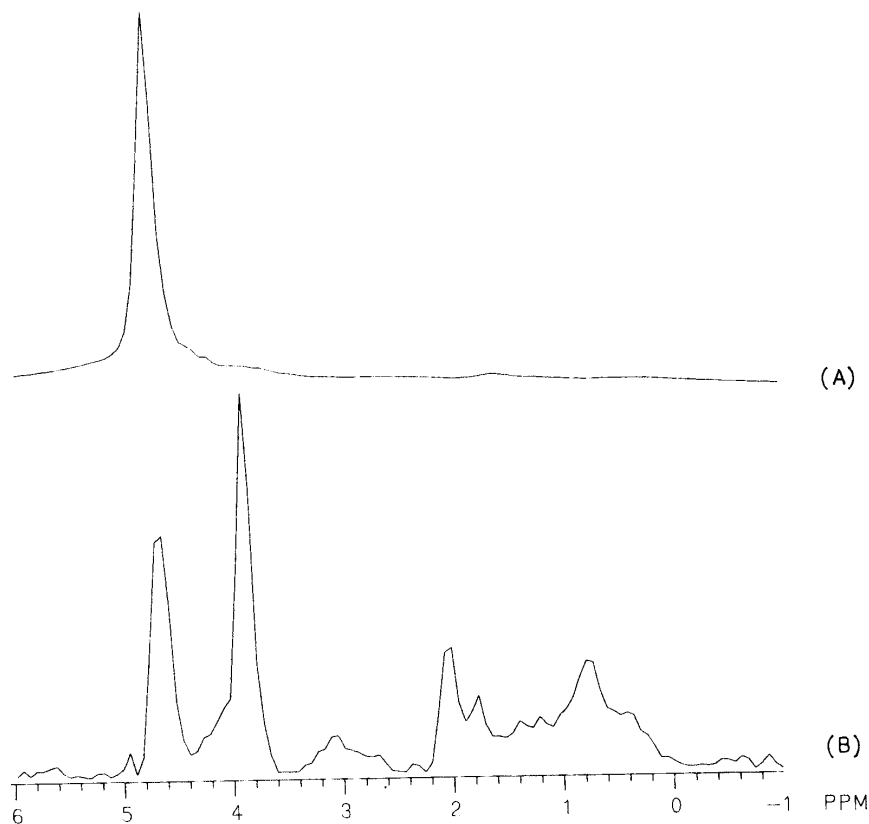


FIG. 10. (A) Proton spectrum of the FID obtained in two excitations from the spectroscopic volume of interest defined in Fig. 9. This spectrum was used to adjust the magnetic field homogeneity to 0.12 ppm. (B) Solvent suppressed proton spectrum obtained using the acquisition parameters as described in text. Note peak consistent with *N*-acetyl aspartate at 2.0 ppm.

TE pulse sequence with an echo time of 500 ms and a recycle time of 2 s. The  $90^\circ$  pulse was a  $1-\tau-\bar{3}-\tau-\bar{3}-\tau-\bar{1}$  solvent suppression pulse with a  $\tau$  of 3 ms and an  $\alpha$  pulse width of  $50 \mu\text{s}$  ( $1 = 50 \mu\text{s}$ ). This spectrum was acquired by averaging 200 excitations. The spectral width was 4 kHz, 1K data points were collected, and a magnitude calculation was performed. The proton image and the solvent suppressed proton spectrum were acquired using the body coil as the excitation coil and the doubly tuned LGR as the receive coil. Figure 11 shows the  $^{31}\text{P}$  NMR spectrum acquired from a 12.5-mm-thick phosphorous slice centered in the same position as that in Fig. 9, 4 cm from a 7.5-cm doubly tuned surface coil. This spectrum was acquired by averaging 200 excitations at a 4-s recycle time using a 4-kHz spectral width and 1K data points, in addition to a 10-Hz exponential line broadening filter.

#### DISCUSSION

The double-resonance loop-gap resonators described possess several characteristics which are useful for *in vivo*  $^1\text{H}$  imaging and gradient-localized  $^{31}\text{P}$  and  $^1\text{H}$  spectroscopy, as described above. The ability to function in any orientation within externally applied excitation fields is particularly valuable for performing MRI/MRS studies on clinical

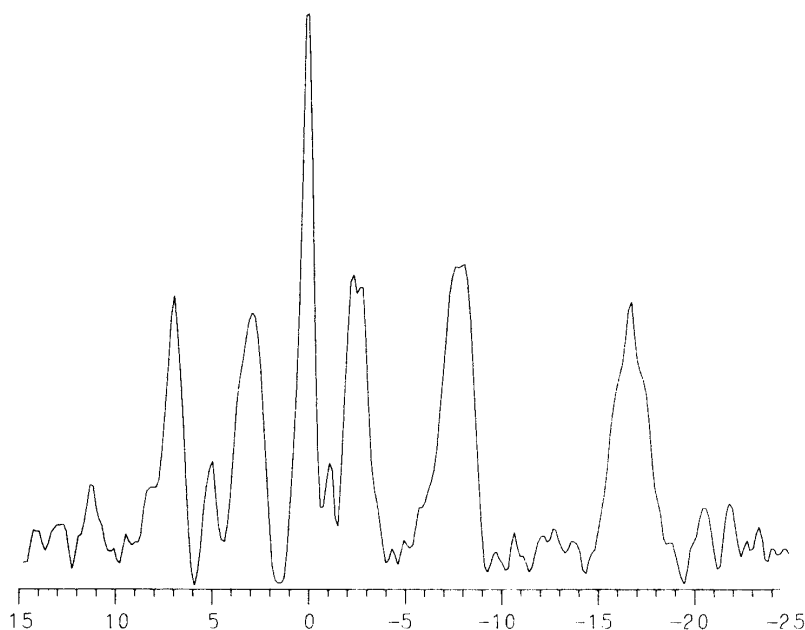


FIG. 11. Phosphorous spectrum from the same volume as that defined in Fig. 9. Acquisition parameters as described in text.

MR systems because there is no need to alter the  $^1\text{H}$  system coils. One group has described a doubly tuned coil design which operates in an externally applied excitation field; however, electrical isolation is achieved simply by maintaining geometric orthogonality between coils (15).

We are currently performing image-localized  $^1\text{H}/^{31}\text{P}$  spectroscopy of the kidney in renal transplant recipients in addition to gated cardiac  $^{31}\text{P}$  MR studies in humans on a regular basis in 60 min or less. This is in part due to the ability to image, shim, and acquire spectra without moving the patient or changing coils. Studies of muscle are performed in less time due to the higher concentrations of metabolites *in vivo*.

The sensitivity of each mode of the doubly tuned resonator is determined by the separation between the loops and the proximity of the loops to the sample. As the separation between the loops is decreased, the sensitivity of the low-frequency mode increases because joulean losses in both loops are dominated by eddy current losses in the sample. The sensitivity of the high-frequency mode, however, decreases because the induced magnetic fields give rise to EMFs in the loops which tend to cancel more effectively. Therefore, by varying the separation between the loops for the geometry shown here, one may optimize the sensitivity for either mode individually or achieve a compromise between both modes.

In this application the low-frequency mode corresponds to the low-sensitivity nucleus. Therefore the separation of the loops was chosen to preserve sensitivity of this mode at the expense of increased cancellation of signals in the high-frequency mode of the resonator. This accounts for the measured 20% loss in sensitivity of the high-frequency mode.

The unexpected 20% gain in SNR of the double-resonance loop-gap resonator in comparison with a comparable singly tuned dual coaxial  $^{31}\text{P}$  coil is inconsistent with

bench-test data and is felt to be multifactorial. Factors which may influence the NMR measured signal-to-noise ratios include (1) the presence of active PIN diode decoupling circuitry in the singly tuned coil or (2) slightly different excitation fields, and therefore volumes of interest, as suggested by a small difference in the linewidths of the spectra. Of related note is the potential utility of the linear excitation field gradient over the region of the receiver coil, which may be desirable for spectroscopic rotating frame imaging (16).

Here the principles of intrinsic decoupling have been shown to be quite useful in developing coils with multiple resonance modes. The concepts have been effective for CRC coils from 2 to 10 cm in diameter and for planar-pair coils. Equally effective double-resonance coils have been built for  $^{23}\text{Na}/^1\text{H}$  and  $^{31}\text{P}/^{19}\text{F}$  at 1.5 T. In addition, similar principles have been used to develop quadrature detection local coils for MR imaging and spectroscopy (18).

#### ACKNOWLEDGMENTS

This work was supported by Grants RR01008 and CA41464 from the National Institutes of Health and a grant from General Electric Medical Systems.

#### REFERENCES

1. D. I. HOULT, S. J. W. BUSBY, D. G. GADIAN, G. K. RADDI, R. E. RICHARDS, AND P. J. SEELEY, *Nature (London)* **952**, 285 (1974).
2. P. A. BOTTOMLEY, T. H. FOSTER, AND R. D. DARROW, *J. Magn. Reson.* **59**, 338 (1984).
3. W. P. AUE, S. MUELLER, T. A. CROSS, AND J. SEELIG, *J. Magn. Reson.* **56**, 350 (1984).
4. R. J. ORDIDGE, A. CONNELLY, AND J. A. B. LOHMAN, *J. Magn. Reson.* **66**, 283 (1986).
5. V. R. CROSS, R. K. HESTER, AND J. S. WAUGH, *Rev. Sci. Instrum.* **47**, 1486 (1976).
6. F. D. DOTY, R. R. INNERS, AND P. D. ELLIS, *J. Magn. Reson.* **43**, 399 (1981).
7. M. D. SCHNALL, V. HARIHAR SUBRMANIAN, J. S. LEIGH, JR., L. GYULAI, A. MCCLAUGHLIN, AND B. CHANCE, *J. Magn. Reson.* **63**, 401 (1985).
8. J. A. DEN HOLLANDER, K. L. BEHAR, AND R. G. SCHULMAN, *J. Magn. Reson.* **57**, 311 (1984).
9. T. A. CROSS, S. MÜLLER, AND W. P. AUE, *J. Magn. Reson.* **62**, 87 (1985).
10. M. O. LEACH, A. J. HIND, J. C. SHARP, R. SAUTER, H. REQUARDT, AND H. WEBER, *Med. Phys.* **13**(4), 510 (1986).
11. T. M. GRIST AND J. S. HYDE, *J. Magn. Reson.* **61**, 571 (1985).
12. J. S. HYDE, W. FRONCISZ, A. JESMANOWICZ, AND J. B. KNEELAND, *Med. Phys.* **13**, (1986).
13. W. FRONCISZ, A. JESMANOWICZ, J. B. KNEELAND, AND J. S. HYDE, *Magn. Reson. Med.* **3**, 590 (1986).
14. W. FRONCISZ, A. JESMANOWICZ, AND J. S. HYDE, *J. Magn. Reson.* **66**, 135 (1986).
15. W. A. EDELSTEIN, C. J. HARDY, AND O. M. MUELLER, "Abstracts SMRM Fourth Annual Meeting, Aug. 19-23, 1985," p. 1084, 1985.
16. L. BOLINGER, M. G. PRAMMER, M. D. SCHNALL, J. C. HASELGROVE, B. CHANCE, AND J. S. LEIGH, "SMRM 1986," p. 208.
17. HOULT, D. I., *J. Magn. Reson.* **33**, 183 (1979).
18. J. S. HYDE, A. JESMANOWICZ, T. M. GRIST, W. FRONCISZ, AND J. B. KNEELAND, *Magn. Reson. Med.* **4**, 179 (1987).